Pergamon

Geochimica et Cosmochimica Acta, Vol. 58, No. 7, pp. 1795–1811, 1994

0016-7037/94 $6.00 + .00

The behavior of scavenged isotopes in marine anoxic environments: ^{210}Pb and ^{210}Po in the water column of the Black Sea

CHING-LING WEI* and JAMES W. MURRAY
School of Oceanography, University of Washington, Seattle, WA 98195, USA

(*Received May* 16, 1992; *accepted in revised form December* 23, 1993)

Abstract—Vertical profiles of dissolved and particulate ^{210}Pb and ^{210}Po were determined at two stations in the Black Sea in June 1988. Vertical fluxes of ^{210}Pb and ^{210}Po were also measured in the upper 150 m, using floating sediment traps.

The fractionation of ^{210}Pb between dissolved and particulate phases in the Black Sea is strongly influenced by the redox conditions in the water column. Dissolved ^{210}Pb dominates in the oxic zone, while particulate ^{210}Pb is the major form in the deep sulfide-rich anoxic zone. The distribution of ^{210}Pb across the suboxic zone appears to be mainly controlled by redox cycling of manganese and iron. In the sulfide-rich layer coprecipitation of lead with iron sulfide is probably the dominant scavenging mechanism.

A simple scavenging model was used to calculate the residence times of dissolved and particulate ^{210}Pb in the oxic, suboxic, and anoxic zones. The residence times of dissolved ^{210}Pb relative to scavenging by particles are 0.5–1, 2–3, and 3.5 years in the oxic, suboxic, and anoxic layers, respectively. The corresponding residence times of particulate ^{210}Pb relative to particle removal processes in the same layers are 0.1, 1.5–2.5, and 8.5 years, respectively. A particle settling velocity of about 40 m y^{-1} was derived from the ^{210}Pb/^{226}Ra disequilibrium in the deep Black Sea. The relatively short residence times of ^{210}Pb support the hypothesis that anoxic basins are important sites for boundary scavenging of ^{210}Pb.

The ^{210}Po profiles indicate that biological rather than inorganic particles are the major carrier phases for polonium in the Black sea. Dissolved ^{210}Po is deficient relative to dissolved ^{210}Pb in the euphotic zone, suggesting preferential uptake of ^{210}Po over ^{210}Pb by particles residing in that layer. The residence time of dissolved ^{210}Po, with respect to scavenging by particles in the euphotic zone, is about 200 days. Below the mid-depth of the suboxic zone, ^{210}Po is in excess relative to ^{210}Pb, and is thought to originate from shelf and slope sediments.

Based on the magnitude of distribution coefficients (K_D), the relative partitioning of lead, polonium, and thorium to particles found in the oxic and anoxic layers of the Black Sea are Po > Th > Pb and Po = Pb > Th, respectively. The dependency of K_D on particle concentration suggests that colloidal phases may be important for the scavenging of these radionuclides.

INTRODUCTION

THE GEOCHEMICAL DISTRIBUTIONS of trace metals have been predicted and shown to vary from oxic to sulfidic environments, depending on their electronic configuration and resulting class A vs. transition metal, vs. class B behavior (EMERSON et al., 1983; JACOBS and EMERSON, 1982). These intrinsic chemical affinities should also apply to the reactivity of metals with particle surfaces. Class A metals are expected to react more strongly with oxide than sulfide particles. Class B metals should react strongly with sulfides. Of elements normally used to study scavenging from seawater, thorium (^{234}Th) should be a tracer for class A behavior while lead (^{210}Pb), and to a lesser extent polonium (^{210}Po), should tend to display class B behavior. ^{210}Po may also be a tracer for nutrient like behavior (KADKO, 1993).

The Black Sea is an ideal location to study how the distribution and fluxes of ^{234}Th, ^{210}Pb, and ^{210}Po are influenced by oxic and sulfidic environments. The anoxic interface in the Black Sea has been well defined (MURRAY et al., 1989; MURRAY, 1991; IZDAR and MURRAY, 1991; TUGRUL et al., 1992; SAYDAM et al., 1993; MURRAY et al., in press) and consists of an oxic surface layer, a sub-oxic interface layer and anoxic, sulfide rich deep water (CODISPOTI et al., 1991). The distribution and fluxes of ^{234}Th have been presented by WEI and MURRAY (1991). Here we present the dissolved and particulate water column profiles and drifting sediment trap fluxes for ^{210}Pb and ^{210}Po collected during the 1988 Black Sea Expedition.

BACKGROUND

The deviation of the activities of ^{210}Po ($t_{1/2}$ = 138.4 d) and ^{210}Pb ($t_{1/2}$ = 22.2 y) from their secular equilibrium values have been used by marine chemists to determine the removal rates of these radionuclides from the ocean. The residence time of ^{210}Pb, derived from ^{210}Pb/^{226}Ra disequilibria, ranges from a few years in the surface ocean to 50 y in the deep sea (BACON et al., 1976; CRAIG et al., 1973; NOZAKI and TSUNOGAI, 1976; CHUNG and CRAIG, 1983). The distribution of ^{210}Pb in the deep ocean appears to be influenced by boundary scavenging processes. The removal rate of ^{210}Pb is higher in coastal ocean areas with high primary productivity and Mn-rich particles. Reducing conditions, found in anoxic water columns and sediments, have also been proposed to be efficient sites of boundary scavenging for ^{210}Pb (SPENCER et al., 1980, 1981).

Although both ^{210}Po and ^{210}Pb are particle reactive, the geochemical mechanisms that are responsible for their fate in marine environments are different. Previous measurements of ^{210}Po and ^{210}Pb in oxygenated seawater showed that biological uptake may be more important than inorganic adsorption for ^{210}Po scavenging (FISHER et al., 1983;

* *Present Address:* Institute of Oceanography, National Taiwan University, P.O. Box 23-13, Taipei, Taiwan, ROC.

KADKO, 1993), while the opposite is true for ^{210}Pb (BACON et al., 1976; SPENCER et al., 1980; SHANNON et al., 1970).

The scavenging mechanisms of ^{210}Po and ^{210}Pb in anoxic basins are further complicated by the particle recycling resulting from the change in redox conditions from oxic to anoxic seawaters. The most dynamic region in the water column of anoxic basins is found at the oxic/suboxic/anoxic interface layer where manganese and iron are rapidly recycled between oxidized solid and reduced soluble forms (SPENCER and BREWER, 1971; SPENCER et al., 1972; LEWIS and LANDING, 1991). The insoluble iron and manganese oxyhydroxides scavenge particle-reactive elements like lead and thorium, and convey the adsorbed elements downward to the deep layer where they are released back to seawater through reductive dissolution. In addition, Pb(II) can form insoluble solid sulphides, which may result in faster removal of ^{210}Pb from anoxic seawater.

There have been some studies of the distribution of ^{210}Po and ^{210}Pb in anoxic marine environments. BACON et al. (1980) measured the distribution of dissolved and particulate ^{210}Pb and ^{210}Po in the anoxic Cariaco Trench. They found the Cariaco Trench to be an effective sink for ^{210}Pb. Excess ^{210}Po activities were present in the upper 300 m, probably reflecting a source at the boundaries of the basin. TODD et al. (1986) presented profiles of dissolved ^{210}Po, ^{210}Pb, and ^{226}Ra from the Orca Basin in the Gulf of Mexico. One of their most striking results was the extremely high activity of ^{210}Po, ^{210}Pb, and ^{226}Ra found at the oxic/anoxic interface. They suggested that recycling of Mn and Fe oxyhydroxides and decomposition of biogenic particles were both responsible for these anomalously high activities. HARADA et al. (1989) also observed excess ^{210}Po in sulfide containing groundwater samples. They proposed that polonium cycling was related to the sulfur cycle.

The oxic/suboxic/anoxic interface in the Black Sea can be described in terms of a sequence of oxidation-reduction reactions involving oxygen and species of nitrogen, sulfur, carbon, manganese, and iron (TUGRUL et al., 1992; SAYDAM et al., 1993; MURRAY et al., 1994). While characteristic features in the water column profiles occur at different depths at different locations, they tend to always be associated with the same density layer (VINOGRADOV and NALBANDOV, 1990; VINOGRADOV, 1991). MURRAY et al. 1994 summarized the density values of the main water column features in the 1988 R/V Knorr pump cast dataset and these are given in Table 1. Here the distributions of ^{210}Pb and ^{210}Po will be discussed in terms of density rather than depth. This will make it easier to compare data from different stations and to discuss the distributions in terms of reaction zones. This approach removes the variability due to the natural oscillations in time and space of the depth of different density surfaces.

METHODS

Seawater was collected using 30 L Niskin bottles mounted on a CTD rosette during R/V *Knorr* cruise 134 to the Black Sea in June 1988 (MURRAY and IZDAR, 1989). All of the Niskin bottles had Teflon coated stainless steel springs. The locations of two sampling stations are shown in Fig. 1. Station BS3-2 was near the center of the western gyre, and BS3-6 was in the middle of the Black Sea between the eastern and western gyres. About 18 L of each sample was pressure filtered (at 12 p.s.i.) through preweighed 0.45 μm Nuclepore filters. The manifold of the N_2 gas line was connected directly to the Niskin bottle to form a closed system to prevent contact between the sample and air. This prevents oxidation of those samples taken from the H_2S containing layer. Filtration was typically completed within one to three hours. The Nuclepore filters were rinsed with 20 mL of deionized water under slight vacuum to remove seasalt and stored in a petri dish for later analyses of particulate ^{210}Pb and ^{210}Po. Samples for ^{226}Ra analyses were collected using 270 L stainless steel Gerard barrels or 30 L Niskin bottles. Samples were processed on board ship, according to the MnO_2 coated fiber method of MOORE (1976). The MnO_2 fibers were stored in plastic bags for later analyses and the results were reported by O'NEILL et al. (1992).

The filtrate from the ^{210}Pb/^{210}Po sample was acidified with about 20 mL concentrated HCl and spiked with 2.2 dpm of ^{209}Po (ORNL P-209), stable lead, and 50 mg of Fe carrier. The samples were bubbled vigorously with compressed air for at least 12 h to achieve isotopic equilibration and to purge H_2S(g) from the sulfide-containing sam-

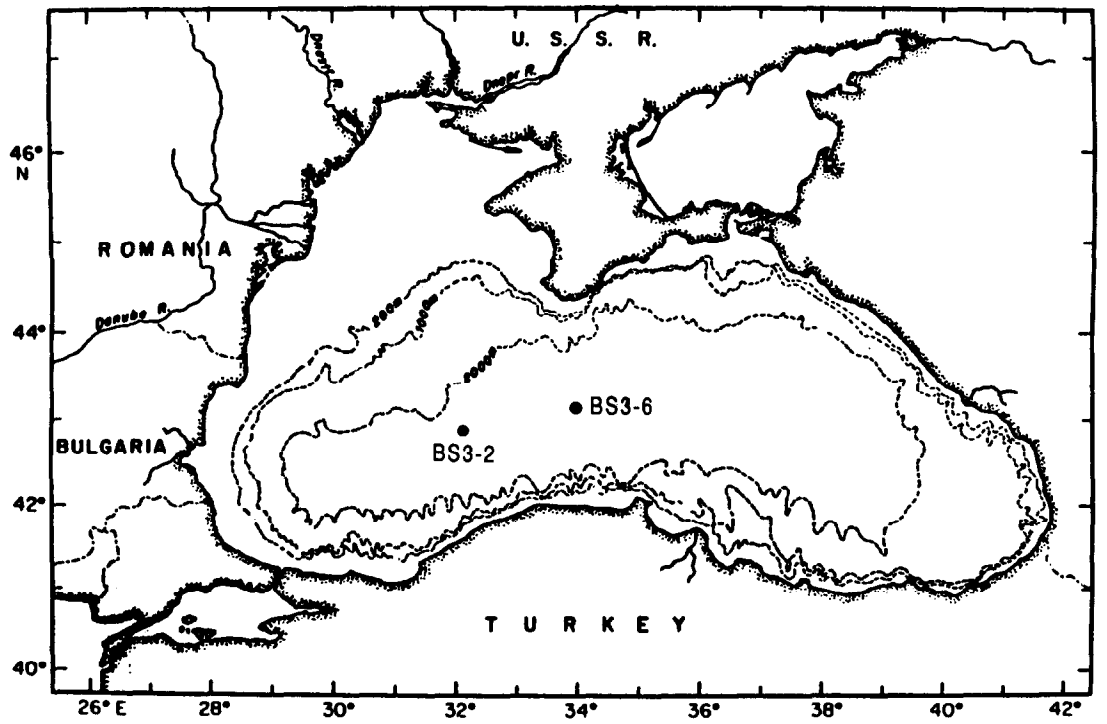

FIG. 1. Map of the Black Sea with the locations of the two sampling stations, BS3-2 and BS3-6, during Leg III of the 1988 Knorr Black Sea Expedition. The nominal station coordinates were BS3-2; 42°50'N, 32°00'E; BS3-6: 43°04'N, 34°00'E.

Table 1. Density (σ_t) values of characteristic features in the water column profiles determined from the 1988 R/V Knorr pump profile data. The density values of all of these features except the shallow PO_4 maximum have a range of about 0.05 density units.

FEATURE	DENSITY
PO_4^{3-} shallow maximum	15.50 (broad density range)
$O_2 < 10$ μM	15.65
NO_3^- maximum	15.40
$Mn_d < 200$nM	15.85
Particulate Mn maximum	15.85
PO_4^{3-} minimum	15.85
NO_2^- maximum	15.85
$NO_3^- < 0.2$ μM	15.95
$NH_4^+ > 0.2$ μM	15.95
$Fe_d < 10$ nM	16.00
$H_2S > 1$ μM	16.15
PO_4 deep maximum	16.20

ples. Concentrated NH_4OH was then added to raise the pH to about 8 to precipitate $Fe(OH)_3$. The $Fe(OH)_3$ precipitate was centrifuged and stored in polypropelyene bottles for analyses in the lab.

The $Fe(OH)_3$ precipitate was dissolved in HCl acid, digested with HNO_3, and ^{210}Po and ^{209}Po were spontaneously plated onto 1 cm^2 silver plates following FLYNN (1968). The particulate samples collected on the Nuclepore filters were dried in a desiccator and weighed to estimate the concentration of total suspended matter (TSM). The filters were then decomposed and digested following the procedures of ANDERSON and FLEER (1982). The ^{210}Po and ^{209}Po were plated onto silver discs. HARADA et al. (1989) have shown that in some types of samples the ^{209}Po tracer does not equilibrate fully with the natural ^{210}Po, and that some of the natural polonium fails to coprecipitate with iron. For this reason, our results should be considered Fe-scavengable polonium.

The sample solutions were stored for at least 1 y to let ^{210}Po grow in from ^{210}Pb. About 2.5 dpm ^{208}Po, which was calibrated against the ^{209}Po standard used in the first plating, was added into the solution and all the three polonium isotopes were plated onto a silver disc. The addition of ^{208}Po yield tracer prevents contamination from the residual ^{209}Po and ^{210}Po activities which were not quantitatively removed from the samples during the initial plating. In fact, all the silver discs from the second plating were found to have a significant amount of residual ^{210}Po.

The silver discs were counted by alpha spectrometry (EG&G Ortec 576). The chemical yield of ^{210}Pb was determined by measuring stable lead using flame atomic absorption spectrophotometry. The ranges of chemical yield for lead are about 80% for dissolved samples and >97% for particulate samples. The procedures used to calculate the activities of ^{210}Po and ^{210}Pb can be found in WEI (1990).

Modified Moss Landing Marine Lab (MLML) pit-type sediment traps (KNAUER et al., 1979; MARTIN et al., 1987) were deployed on a free-floating mooring line at locations near the water column sampling stations, BS3-2 and BS3-6. The sediment traps were deployed at three depths (40, 75, and 150 m) to get direct measurements of the vertical fluxes of total mass, ^{210}Pb and ^{210}Po in the chemically contrasting oxic, suboxic, and anoxic zones. Each trap had a cross-sectional area of about 50 cm^2. The duration of deployment at each station was about three days.

The trap solutions were prepared by adding about 800 g of NaCl and about 60 mL of 37% formaldehyde to 20 L of filtered (0.45 μm Millipore) subsurface seawater taken near the trap deployment locations. The trap solutions used for the deep sediment traps, deployed in the sulfide-containing seawater, were bubbled overnight using N_2 gas to remove oxygen. Upon recovery, the upper layer of seawater in the traps was siphoned off and the remaining trap solution was gravity-drained through a preweighed 47 mm Nuclepore filter (0.45 μm pore size) mounted on the bottom of the trap. The filters were rinsed with about 10 mL of deionized water, under a slight vacuum, to remove sea salt. Zooplankton swimmers were carefully picked by hand. Only the traps deployed in the oxic zone were found to have zooplankton swimmers and there were less than ten per trap. The filters were dried in a desiccator at room temperature and weighed to estimate the total mass flux. Three trap samples from each depth were combined for the analyses of ^{210}Pb and ^{210}Po. Total ^{210}Po and ^{210}Pb activities on the trap filters were determined by the same procedures used for the particulate samples.

RESULTS

The concentrations of total suspended matter and activities of dissolved and particulate ^{210}Pb and ^{210}Po at stations BS3-2 and BS3-6 are given in Table 2. The hydrographic and nutrient data from CTD and pump casts are available in WHITE et al. (1989) and CODISPOTI and FRIEDERICH (1991). One of the striking findings from the 1988 Knorr expedition to the Black Sea was the ubiquitous suboxic zone ($[O_2] < 10$ μM). The depth ranges of the suboxic zone observed at BS3-2 and BS3-6 were 50–95 m and 70–120 m, respectively. The density range was the same for both stations and extended from sigma-t = 15.65, where O_2 decreased to less than 10 μM, to sigma-t = 16.15, where H_2S increased to greater than 1 μM (Table 1). Throughout this paper, oxic, and anoxic zones (H_2S zone) are designated to represent the water column above and below the suboxic zone.

Dissolved and Particulate ^{210}Pb

Dissolved and particulate ^{210}Pb and ^{210}Po and total suspended matter are plotted vs. density in Figs. 2 and 3. The upper and lower boundaries of the suboxic zone are indicated in the figures. Dissolved ^{210}Pb is enriched in the surface water of both BS3-2 and BS3-6. The activity of dissolved ^{210}Pb decreases from the oxic to the anoxic layer. At BS3-2 dissolved ^{210}Pb decreases continuously across the suboxic zone to a low activity (<1 dpm 100 L^{-1}) near the suboxic/anoxic boundary, while at BS3-6 it has a small maximum in the middle

Table 2. Depth, cast number, potential density, total suspended matter (TSM) concentration, dissolved (DPb) and particulate (PPb) ^{210}Pb, and dissolved (DPo) and particulate (PPo) ^{210}Po collected in June 1988 from the Black Sea. Standard deviation are based on propagated counting error. (± 1σ).

Depth m	Cast #	Sigma Theta	TSM mg/l	DPb dpm/100 l	PPb dpm/100 l	DPo dpm/100 l	PPo dpm/100 l
BS3-2							
10	H1	13.19	0.57	11.90± 0.51	1.17± 0.08	2.20± 0.12	1.57± 0.13
20	H1	13.71	0.25	7.74± 0.34	0.36± 0.02	1.94± 0.09	0.31± 0.04
30	H1	14.02	0.24	21.88± 1.10	0.52± 0.03	15.05± 0.89	0.57± 0.05
40	H4	14.67	0.12	7.74± 0.42	1.29± 0.07	2.40± 0.12	0.62± 0.06
45	H4	14.91	0.13	4.41± 0.25	1.68± 0.08	2.53± 0.12	5.96± 0.29
50	H4	15.28	0.16	2.77± 0.15	1.74± 0.09	1.50± 0.07	4.12± 0.25
55	H6	15.41	0.04	4.42± 0.22	1.37± 0.08	2.18± 0.10	19.18± 0.91
60	H6	15.45	-	3.37± 0.18	-	2.06± 0.10	-
65	H6	15.71	0.06	3.35± 0.20	1.73± 0.10	3.89± 0.17	29.48± 1.53
70	H9	15.82	0.11	2.67± 0.16	0.65± 0.04	2.89± 0.14	11.69± 0.67
75	H9	15.95	0.12	1.96± 0.11	0.73± 0.04	1.11± 0.05	11.28± 0.62
80	H9	15.99	0.17	2.04± 0.12	1.01± 0.06	4.29± 0.21	10.53± 0.62
85	H12	16.11	0.15	0.64± 0.05	2.34± 0.11	3.90± 0.20	8.31± 0.52
90	H12	16.13	0.11	0.82± 0.05	2.61± 0.16	3.77± 0.20	11.40± 0.54
95	H12	16.21	0.10	0.92± 0.05	3.53± 0.19	3.54± 0.16	15.11± 0.56
100	H13	16.26	0.01	0.94± 0.05	2.79± 0.15	2.79± 0.23	13.21± 0.51
105	H13	16.28	0.06	0.86± 0.05	2.95± 0.14	2.99± 0.15	25.33± 0.77
110	H13	16.28	0.03	1.13± 0.06	3.31± 0.19	3.44± 0.21	12.85± 0.41
115	H16	16.36	0.05	0.55± 0.03	3.41± 0.22	2.58± 0.14	20.33± 0.71
120	H16	16.39	0.04	0.50± 0.03	2.61± 0.14	2.36± 0.15	6.34± 0.35
130	H16	16.44	0.09	0.58± 0.04	2.74± 0.14	2.91± 0.17	7.70± 0.48
140	H17	16.49	0.06	0.82± 0.04	2.22± 0.10	4.10± 0.43	5.18± 0.31
170	H17	16.60	0.11	0.88± 0.05	2.49± 0.13	2.16± 0.16	7.60± 0.51
200	H17	16.69	0.06	0.86± 0.04	2.33± 0.12	2.00± 0.11	4.37± 0.29
400	H18	16.97	0.07	1.21± 0.06	2.34± 0.13	2.67± 0.22	7.61± 0.46
600	H18	17.10	0.06	1.31± 0.08	2.55± 0.13	2.25± 0.13	5.15± 0.33
800	H18	17.17	0.08	1.21± 0.06	3.04± 0.17	3.30± 0.16	5.33± 0.31
1200	H20	17.21	0.04	1.20± 0.06	2.43± 0.13	2.21± 0.21	3.53± 0.19
1600	H20	17.22	0.14	1.27± 0.07	2.77± 0.15	2.35± 0.19	5.15± 0.24
2076	H20	17.22	0.05	2.97± 0.15	2.12± 0.11	3.22± 0.29	13.06± 0.76
BS3-6							
5	H17	12.50	0.19	6.98± 0.39	0.78± 0.05	3.98± 0.31	13.47± 0.72
15	H17	13.43	0.16	5.51± 0.31	0.74± 0.05	1.69± 0.13	7.33± 0.38
30	H17	14.16	0.21	4.80± 0.24	0.50± 0.04	3.06± 0.25	9.08± 0.42
50	H14	14.72	0.07	1.49± 0.09	1.17± 0.09	1.03± 0.10	2.09± 0.10
65	H14	15.38	0.10	0.97± 0.08	0.43± 0.03	0.61± 0.04	2.24± 0.12
70	H14	15.56	0.07	0.65± 0.05	0.24± 0.02	0.60± 0.06	2.69± 0.15
75	H12	15.62	0.10	1.44± 0.10	0.54± 0.03	0.61± 0.08	1.70± 0.09
80	H12	15.74	0.18	0.76± 0.06	0.60± 0.04	0.38± 0.06	2.66± 0.14
85	H12	15.86	0.05	1.01± 0.07	0.53± 0.03	0.56± 0.06	2.00± 0.10
90	H10	15.93	0.04	2.41± 0.14	0.26± 0.02	0.78± 0.08	5.77± 0.34
95	H10	15.99	0.06	1.49± 0.11	0.19± 0.02	1.02± 0.10	5.09± 0.28
100	H10	16.08	0.07	1.28± 0.10	0.93± 0.06	1.17± 0.12	7.72± 0.46
105	H9	16.08	0.07	1.22± 0.08	0.85± 0.06	0.79± 0.09	3.06± 0.21
110	H9	16.14	0.09	0.67± 0.07	1.56± 0.09	2.06± 0.22	4.90± 0.21
115	H9	16.20	0.07	0.87± 0.06	2.03± 0.13	1.92± 0.25	4.75± 0.21
120	H7	16.27	0.07	0.83± 0.07	2.66± 0.16	1.59± 0.14	4.08± 0.22
125	H7	16.31	0.06	0.60± 0.06	2.66± 0.21	2.26± 0.21	4.35± 0.22
130	H7	16.33	0.07	0.56± 0.05	2.48± 0.15	1.57± 0.54	4.97± 0.32
150	H5	16.43	0.07	0.73± 0.07	2.48± 0.16	2.17± 0.79	5.56± 0.29
180	H5	16.55	0.07	0.88± 0.08	2.19± 0.12	1.56± 0.17	6.26± 0.23
250	H5	16.74	0.06	1.06± 0.09	1.70± 0.12	2.57± 0.14	3.98± 0.18
500	H3	17.02	0.03	0.86± 0.06	2.54± 0.15	2.51± 0.18	4.74± 0.25
800	H3	17.16	0.04	1.82± 0.20	2.19± 0.13	2.02± 0.20	5.69± 0.22
1500	H3	17.22	0.04	1.27± 0.21	2.62± 0.17	2.28± 0.30	5.25± 0.32
2155	H1	17.221	0.03	1.15± 0.08	2.25± 0.14	2.43± 0.16	3.62± 0.20
2165	H1	17.221	0.03	1.50± 0.10	2.38± 0.15	2.08± 0.15	7.40± 0.46
2175	H1	17.221	0.02	1.25± 0.08	2.57± 0.16	2.22± 0.14	10.53± 0.51

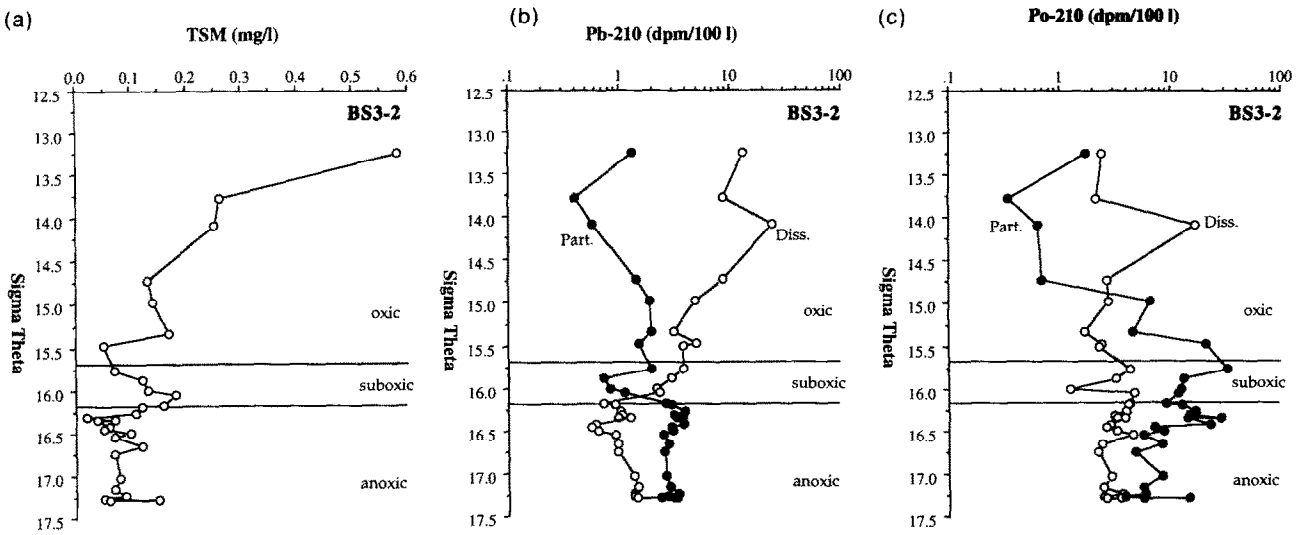

FIG. 2. Vertical distributions vs. density (sigma theta) of (a) total suspended matter (TSM) and (b) dissolved (open circles) and particulate (solid circles) ^{210}Pb, and (c) dissolved (open circles) and particulate (solid circles) ^{210}Po at BS3-2. The uncertainties, based on the propagation of counting errors, are smaller than the symbols. The upper and lower boundaries of the suboxic zone are represented by the horizontal lines.

of the suboxic zone. Dissolved ^{210}Pb increases slightly with density in the deep sulfide layer.

Overall, the vertical profiles of particulate ^{210}Pb show a mirror image to those of dissolved ^{210}Pb. From the surface to the bottom boundary of the suboxic zone, the particulate ^{210}Pb activities are lower (<2 dpm 100 L^{-1}) than the dissolved ^{210}Pb activities. There are two common features in the distribution of particulate ^{210}Pb at both stations. There is a minimum at sigma-t = 16.0 ± 0.1, which is about the density where dissolved Mn (σ_t = 15.85) and Fe (σ_t = 16.00) start to increase rapidly. There is a broad maximum, of small magnitude, centered at σ_t = 16.30 ± 0.05 which is just below the first appearance of sulfide at σ_t = 16.15. The crossover between dissolved and particulate ^{210}Pb occurs at the bottom of the suboxic zone.

Except for a single point near the seawater-sediment interface at BS3-2, all the particulate ^{210}Pb activities in the deep water exceed the dissolved ^{210}Pb activities, and the particulate ^{210}Pb in the deep H_2S zone shows a relatively constant activity of about 2.5 dpm 100 L^{-1}.

Dissolved and Particulate ^{210}Po

The activities of dissolved ^{210}Po are less than those of dissolved ^{210}Pb in the surface euphotic zone at both stations. This deficiency exists to the depth of the upper layer of the

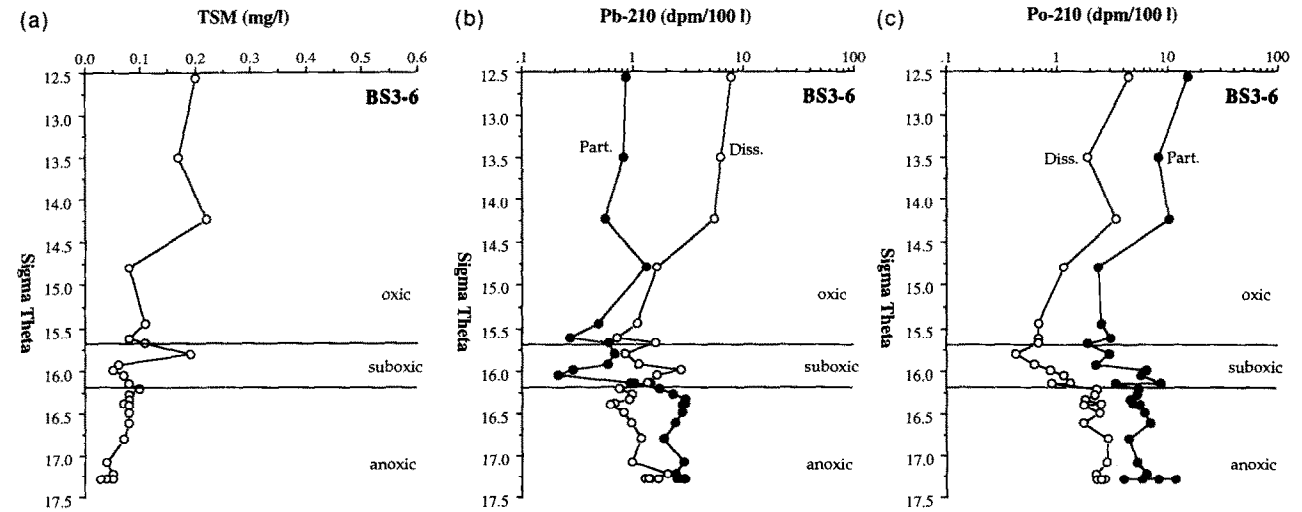

FIG. 3. Vertical distributions vs. density (sigma theta) of (a) total suspended matter (TSM), (b) dissolved (open circles), and particulate (solid circles) ^{210}Pb, and (c) dissolved (open circles) and particulate (solid circles) ^{210}Po at BS3-6. The uncertainties, based on the propagation of counting errors, are smaller then the symbols. The upper and lower boundaries of the suboxic zone are represented by the horizontal lines.

suboxic zone and decreases with increasing density (Figs. 2, 3). Below the lower layer of the suboxic zone, the activity of dissolved ^{210}Po is higher than that of dissolved ^{210}Pb.

There are significant differences in the distribution of particulate ^{210}Po in the oxic and suboxic zones of BS3-2 and BS3-6. At BS3-2, a low particulate ^{210}Po activity (<2 dpm 100 L^{-1}) was observed in the oxic layer and a sharp increase in particulate ^{210}Po was observed at a σ_t of approximately 15.0. Particulate ^{210}Po activity in the suboxic and upper H_2S zones varied from 7 to 30 dpm 100 L^{-1}, and remained higher than dissolved ^{210}Po. There is a maximum in particulate ^{210}Po at σ_t = 16.30. In contrast, at BS3-6, particulate ^{210}Po is enriched in the surface layer (7–13 dpm 100 L^{-1}) then decreases to about 2 dpm 100 L^{-1} in the upper part of the suboxic zone. A small maximum of particulate ^{210}Po, of about 7.5 dpm 100 L^{-1} was observed to be centered at σ_t = 16.15.

At both stations, a relatively constant activity (3–5 dpm 100 L^{-1}) of particulate ^{210}Po was found in the H_2S layer. It should be noted that particulate ^{210}Po tends to increase in the bottom boundary layer. This feature is especially clear from the three samples taken at 10, 20, and 40 m above the bottom sediments at BS3-6.

Fluxes of ^{210}Pb and ^{210}Po in the Upper 150 m

The fluxes of total mass, ^{210}Pb, ^{210}Po, the specific activities of ^{210}Pb and ^{210}Po, and the ^{210}Po/^{210}Pb ratio in trap particles are given in Table 3. Vertical variations of the fluxes of total mass, ^{210}Pb, and ^{210}Po are shown in Fig. 4. The flux data are plotted vs. depth rather than density because the traps were deployed for three days. Equivalent density values can be estimated by comparison with the data in Table 2. Values of the mass flux were obtained from the ^{234}Th traps (WEI and MURRAY, 1992) as well as the ^{210}Pb/^{210}Po traps (Table 3) and all values are shown in Fig. 4a. The mass fluxes are systematically higher at BS3-2 than at BS3-6 by a factor of about 2. The fluxes at BS3-2 exhibited a maximum at 75 m while those at BS3-6 decreased continuously with depth to 150 m. In general, there is excellent agreement between the mass fluxes obtained from the ^{234}Th and ^{210}Pb traps.

The ^{210}Pb fluxes decreased from 13 dpm m^{-2} d^{-1} at 40 m to 9–10 dpm m^{-2} d^{-1} at 150 m. BS3-2 had almost the same ^{210}Pb fluxes as BS3-6. ^{210}Po fluxes show larger variability than those for ^{210}Pb. At BS3-2, a maximum was found in the suboxic zone while the ^{210}Po fluxes at BS3-6 are systematically larger and increased monotonically with depth. In contrast to the total mass fluxes, there was a higher ^{210}Po flux at BS3-6 than BS3-2. It should be noted that the ^{210}Po fluxes are lower than the ^{210}Pb fluxes in the oxic layer, while in the suboxic and H_2S zones, ^{210}Po fluxes were either equal to or larger than the ^{210}Pb fluxes.

The ^{234}Th fluxes were presented by WEI and MURRAY (1992) and have a depth distribution similar to the ^{210}Po flux at BS3-2. BUESSELER (1991) argued that the measured ^{234}Th fluxes using drifting sediment traps were larger than model-predicted ^{234}Th fluxes by a factor of 2–3 because of overtrapping by the drifting traps. This suggests that the fluxes for ^{210}Pb and ^{210}Po may be upper limits. The good agreement between the mass fluxes for the ^{234}Th and ^{210}Pb traps suggests that if hydrodynamics cause overtrapping, it does not introduce much variability.

DISCUSSION

Effect of Redox State on Partitioning of ^{210}Pb

The fractionation of ^{210}Pb between dissolved and particulate phases in the Black Sea is strongly influenced by the redox condition of the water column (Figs. 2, 3). From the

Table 3. Vertical fluxes of total mass, ^{210}Pb, and ^{210}Po determined from sediment trap samples collected in the Black Sea in June 1988. Standard deviations of total mass fluxes are based on the three measurements from the same depth. Standard deviations of the ^{210}Pb and ^{210}Po activities are calculated as the ratio of ^{210}Pb and ^{210}Po fluxes to total mass fluxes.

BS3-2

Depth m	Mass Flux mg/m2/d	Pb210 Flux dpm/m2/d	Po210 Flux dpm/m2/d	Pb210 dpm/g	Po210 dpm/g	Po210/Pb210
36	588 ± 133	13.2 ± 1.2	9.0 ± 0.5	22.5 ± 5.5	15.3 ± 3.6	0.68
71	731 ± 262	10.8 ± 1.0	12.2 ± 0.5	14.8 ± 5.5	16.7 ± 6.0	1.13
146	363 ± 117	8.7 ± 1.0	8.0 ± 0.4	23.9 ± 8.2	21.9 ± 7.1	0.92

BS3-6

Depth m	Mass Flux mg/m2/d	Pb210 Flux dpm/m2/d	Po210 Flux dpm/m2/d	Pb210 dpm/g	Po210 dpm/g	Po210/Pb210
40	310 ± 46	13.0 ± 1.2	11.7 ± 0.5	42.0 ± 7.3	37.6 ± 5.8	0.89
75	240 ± 66	10.4 ± 1.0	13.6 ± 0.6	43.3 ± 12.7	56.7 ± 15.8	1.31
150	112 ± 8	9.8 ± 1.0	16.6 ± 0.9	87.1 ± 10.8	148.5 ± 13.0	1.71

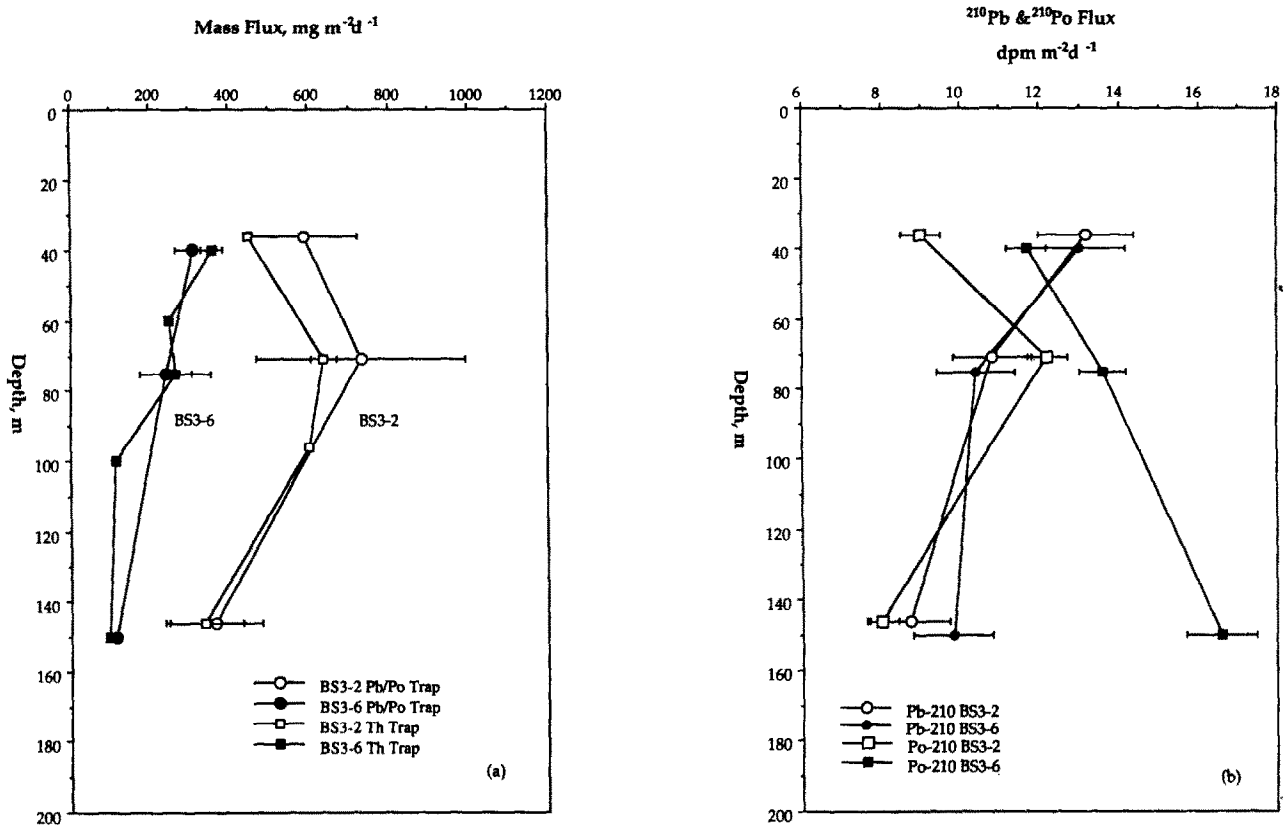

FIG. 4. (a) Vertical profiles vs. depth of total mass fluxes at BS3-2 (open circles) and BS3-6 (solid circles). Mass fluxes from Th traps collected on the same array are also shown (from WEI and MURRAY, 1992). Error bars are standard deviation ($\pm 1\sigma$) of the mass fluxes measured by three traps deployed at the same depth. (b) Vertical profiles vs. depth of ^{210}Pb (circles) and ^{210}Po (squares) fluxes at BS3-2 (open symbols) and BS3-6 (solid symbols). Error bars are the uncertainties based on the propagated counting errors ($\pm 1\sigma$).

surface to the lower portion of the suboxic zone at σ_t = 16.15, ^{210}Pb is mainly found in the dissolved form, while particulate ^{210}Pb dominates the total concentration in the sulfide-containing deep water. This type of distribution was also observed in the Cariaco Trench (BACON et al., 1980); however, particulate ^{210}Pb in the H_2S zone of the Black Sea generally has higher concentrations.

Dissolved ^{210}Pb activities in the oxic and suboxic layers show a significant geographic variation. There is about twice as much dissolved ^{210}Pb in the oxic and suboxic layers at station BS3-2 than at BS3-6. This may be due to differences in horizontal advective transport from the margins of the Black Sea or differences in the scavenging rate. Based on only two profiles, it is difficult to determine which of these is responsible.

The vertical variation of the fraction of ^{210}Pb associated with particulate phases is shown in Fig. 5. In the surface layer only about 10% or less of the ^{210}Pb is filterable. This value is lower than the corresponding value of 20% observed in the Cariaco Trench (BACON et al., 1980). The percentage as particulate ^{210}Pb increases to 20–40% in the upper part of the suboxic zone where the concentrations of particulate manganese and iron are higher. This percentage drops to a minimum at σ_t = 15.95, then increases sharply to values of 80% in the anoxic zone.

Dissolved manganese and iron start to increase at σ_t = 15.85 and σ_t = 16.00, respectively (Table 1), suggesting that the upward flux of dissolved iron is removed at a deeper layer than that of manganese. Changes in the gradient are the best indicators of reaction zones (SHOLKOVITZ, 1992) and the removal zones of dissolved manganese and iron are clearly separated. The slightly elevated concentrations of dissolved manganese and iron above these reaction zones either reflect less than 100% efficient removal of the vertical flux, a horizontal flux from the boundaries, or internal recycling. Potential oxidation rates of Mn(II) were measured by TEBO et al. (1991) and high values were found at all depths in the suboxic zone. Maximum values were observed at σ_t = 16.1 and σ_t = 15.75. Both layers correspond approximately to maxima in particulate manganese (LEWIS and LANDING, 1991). The deeper maximum contains oxidized manganese, however, the shallower maximum does not. TEBO (1991) has shown that manganese oxidation rates are much higher at the margins than in the interior of the basin, but there is no agreement about the relative importance of in situ vs. horizontal transport for creation of either of these maxima (see also KEMPE et al., 1991; LEWIS and LANDING, 1991).

The high concentrations of particulate manganese and iron generally coincide with high particulate ^{210}Pb. The resolution in the dataset is not sufficient to determine whether man-

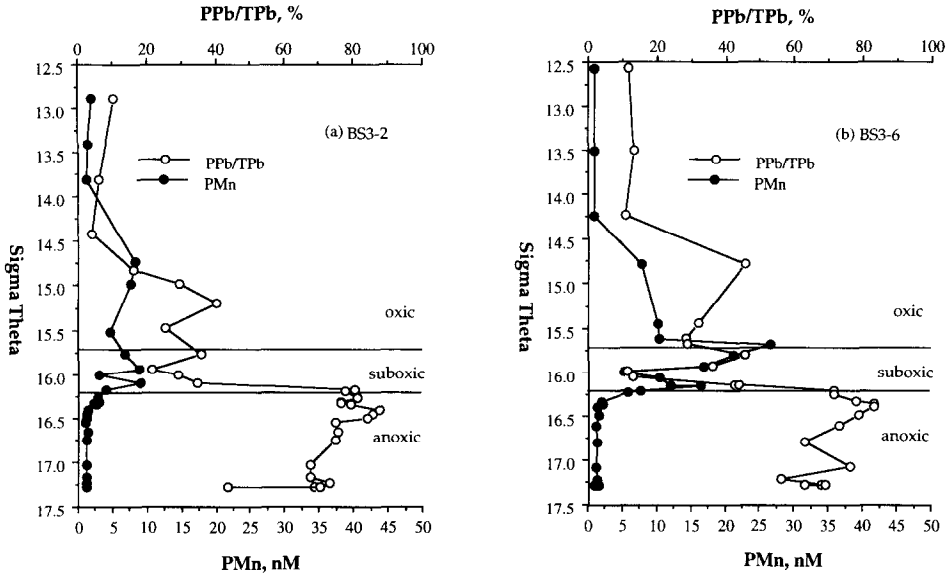

FIG. 5. Vertical distributions vs. density of the ratio of particulate ^{210}Pb to total ^{210}Pb at BS3-2 (a) and BS3-6 (b). The particulate manganese data (PMn) of LEWIS and LANDING (1991) is also shown (solid symbols).

ganese or iron oxides are more important, but it does appear that metal oxide scavenging does play a role in removing dissolved ^{210}Pb. The particulate manganese data (from LEWIS and LANDING, 1991) is shown in Fig. 5. Particulate iron is not shown, because no recycling signal can be seen superimposed on the high background levels.

In the upper part of the sulfide-containing deep water (at σ_t = 16.30) about 80% of the ^{210}Pb is associated with particulate matter. Because of the slight increase of dissolved ^{210}Pb with density (Figs. 2, 3), the ratio of particulate to total (PPb/TPb) decreases from 80% at upper portion of the H_2S zone to 60–70% toward the bottom. In the deep, open ocean, the PPb/TPb ratio is usually less than 0.05 (BACON et al., 1976). This large difference in the fractionation reflects the tendency of lead to adsorb on and/or precipitate as sulfide phases in anoxic waters.

Residence Time of ^{210}Pb

The activity of dissolved ^{210}Pb in seawater is determined by atmospheric ^{210}Pb input, in situ production from ^{226}Ra, radioactive decay, and scavenging processes. In order to derive residence times of dissolved and particulate ^{210}Pb, the atmospheric ^{210}Pb flux and the ^{226}Ra source functions have to be known.

Dissolved ^{210}Pb is enriched in the surface layer and decreases sharply through the pycnocline (Figs. 2, 3). This surface enrichment is typically found in the open ocean, and is a result of atmospheric input (BACON et al., 1976). The influence of atmospheric ^{210}Pb fluxes is limited to the surface layer because of the strong pycnocline, that begins at approximately 40–50 m. There have been no direct measurements of the atmospheric flux of ^{210}Pb to the Black Sea; however, an indirect estimate of the upper limit of this input can be made, as follows.

If we assume the standing stock of ^{210}Pb in the surface layer is maintained at a steady-state concentration, and that riverine and horizontal inputs are negligible, then the atmospheric flux of ^{210}Pb into the Black Sea must be balanced by a flux out of the surface layer. The ^{210}Pb fluxes measured by the sediment traps deployed at 40 m at BS3-2 and BS3-6 were about 13 dpm m^{-2} d^{-1} (0.47 dpm cm^{-2} y^{-1}) (Table 3). This value is comparable to the atmospheric ^{210}Pb flux in other regions at the same latitude (TUREKIAN et al., 1977). Hence, for calculation of the residence times of dissolved and particulate ^{210}Pb in the surface layer, we will assume an atmospheric ^{210}Pb flux of 13 dpm m^{-2} d^{-1}. This should be considered as a first approximation because of the variable distributions and the assumptions stated above.

The in situ production from decay of ^{226}Ra is an important source of ^{210}Pb in the water column, especially for the deep water. The distribution of ^{226}Ra in the Black Sea was determined from the samples taken from cruises 3 and 4 of the 1988 Knorr Expedition (O'NEILL et al., 1992). The average activities of ^{226}Ra in the surface, suboxic, and deep layers of the central basin of the Black Sea are 6, 25, and 15 dpm 100 L^{-1}, respectively.

With the known ^{226}Ra distribution and an estimate of the atmospheric ^{210}Pb flux, a simple, irreversible scavenging model (BACON et al., 1980) was used to calculate the residence times of dissolved and particulate ^{210}Pb in the oxic, suboxic, and anoxic layers using the following equations:

$$\partial \mathrm{DPb}/\partial t = 0 = A + \lambda_{\mathrm{Pb}} I_{\mathrm{Ra}} - \lambda_{\mathrm{Pb}} I_{\mathrm{DPb}} - k_1 I_{\mathrm{DPb}}, \quad (1)$$

$$\partial \mathrm{PPb}/\partial t = 0 = k_1 I_{\mathrm{DPb}} - \lambda_{\mathrm{Pb}} I_{\mathrm{PPb}} - k_2 I_{\mathrm{PPb}}, \quad (2)$$

$$k_1 = (\lambda_{\mathrm{Pb}}(I_{\mathrm{Ra}} - I_{\mathrm{DPb}}) + A)/I_{\mathrm{DPb}}, \quad (3)$$

$$k_2 = (k_1 I_{\mathrm{DPb}} - \lambda_{\mathrm{Pb}} I_{\mathrm{PPb}})/I_{\mathrm{PPb}}, \quad (4)$$

$$\tau_{\mathrm{DPb}} = 1/k_1, \quad (5)$$

$$\tau_{\mathrm{PPb}} = 1/k_2, \quad (6)$$

where

I_{Ra}, I_{DPb}, I_{PPb} = Inventories of ^{226}Ra, dissolved ^{210}Pb, particulate ^{210}Pb,
λ_{Pb} = Decay constant of ^{210}Pb (0.0312 y^{-1}),
A = Atmospheric ^{210}Pb flux (4745 dpm m^{-2} y^{-1} for the surface box and 0 for the suboxic and anoxic boxes),
k_1, k_2 = Scavenging and removal rate constants of dissolved ^{210}Pb and particulate ^{210}Pb (y^{-1})
τDPb, τPPb = Residence time of dissolved ^{210}Pb and particulate ^{210}Pb (y).

The inventories of ^{226}Ra, dissolved ^{210}Pb, particulate ^{210}Pb, and calculated residence times of dissolved and particulate ^{210}Pb are shown in Table 4. These calculations have been made in terms of depth rather than density to coincide with the trap depths. In the surface oxic layer (0–50 m), τDPb is mainly determined by the standing stock of dissolved ^{210}Pb and atmospheric ^{210}Pb flux. If we have overestimated the atmospheric input, the calculated residence time is too high. Only about 2–4% of dissolved ^{210}Pb in the surface layer is produced from the radioactive decay of ^{226}Ra. Residence times of 1.2 and 0.5 y are obtained for dissolved ^{210}Pb in the surface layer of BS3-2 and BS3-6, respectively. The average τDPb of 0.8 y is shorter than the τDPb of 2.5 y observed for the open ocean (BACON et al., 1976), and is probably due to the larger particulate loads at this time of year in the Black Sea.

It is interesting that τPPb in the surface layer is short (0.1 y) relative to τDPb. This implies that the overall rate of removal of ^{210}Pb from the surface layer of the Black Sea is determined by adsorption or uptake by particles, rather than particle removal. The short value of τPPb is consistent with the residence times of total suspended matter and particulate ^{234}Th, reported previously (WEI and MURRAY, 1992).

The τDPb in the suboxic layers of BS3-2 and BS3-6 are 3.3 and 1.9 y, respectively. The shorter τDPb for BS3-6 may be a result of more scavenging phases in the suboxic layer. This is supported by the observation that particulate Mn in the suboxic zone is several times larger at BS3-6 than at BS3-2 (Fig. 5) (LEWIS and LANDING, 1991). The residence times of particulate ^{210}Pb are in the suboxic layer (2.6 and 1.5 y for BS3-2 and BS3-6, respectively) are of the same magnitude as those of dissolved ^{210}Pb. Thus, within the suboxic zone, it takes about equal time for ^{210}Pb to be scavenged onto the particulate phases and for the adsorbed ^{210}Pb to be removed.

Ventilation of the oxic and suboxic layers is thought to be rapid and occur, at least partially, on a timescale of less than one year (BUESSELER et al., 1991). The variability in the ^{210}Pb and ^{210}Po profiles in the oxic and suboxic layers is probably due to this process. It is very likely that the steady state assumption used in these calculating residence times is not valid but we lack, at present, the data to evaluate this assumption more rigorously.

CRAIG et al. (1973) postulated that the removal of ^{210}Pb from the oxygenated deep water of the open ocean is limited by the rate of adsorption onto particles. In contrast, TSUNOGAI and NOZAKI (1971) and TSUNOGAI et al. (1974) argued that the adsorption rate of ^{210}Pb onto suspended particles should be a fast process, relative to the residence time of particles. In the deep water of the Black Sea, ^{210}Pb is only about 25% of the secular equilibrium values expected from ^{226}Ra. The residence time of dissolved ^{210}Pb relative to uptake by particles in the deep anoxic zone of the Black Sea is about 3.6 y. The residence time of particulate ^{210}Pb in the deep anoxic zone, relative to the particle removal rate, is about 8.5 y. This is a factor of about 2.3 longer than the τDPb. Hence, the particle settling velocity is the determining process for overall removal of ^{210}Pb in the deep water of the Black Sea.

The residence time of dissolved ^{210}Pb (3.6 y) in the deep water of the Black Sea is comparable to the value of 2 y in the deep Cariaco Trench (BACON et al., 1980), and 1 y in the anoxic hypersaline layer in the Orca Basin (TODD et al., 1986), but is much shorter than the value for the deep open ocean (20–90 y, BACON et al., 1976). The common feature of short dissolved residence times for ^{210}Pb in anoxic basins suggests that the formation of an insoluble metal sulfide phase is an efficient mechanism for removing lead. BACON et al.

Table 4. Results of the residence times of dissolved (τ_{DPb}) and particulate (τ_{PPb}) ^{210}Pb calculated from the mass balance equations and the standing stocks of ^{226}Ra, dissolved ^{210}Pb, and particulate ^{210}Pb.

Station	BS3-2			BS3-6		
Depth(m)	Box 1 (0-50)	Box 2 (50-95)	Box 3 (95-2000)	Box 1 (0-70)	Box 2 (70-120)	Box 3 (120-2000)
I_{Ra} (dpm/m^2)	3770	10770	266520	3770	10770	266520
I_{DPb} (dpm/m^2)	5617	1001	27816	2600	594	26558
I_{DPo} (dpm/m^2)	487	731	50850	513	447	48497
τ_{DPb} (year)	1.2	3.3	3.7	0.5	1.9	3.6
τ_{PPb} (year)	0.1	2.6	8.7	0.1	1.5	8.1

(1980) suggested that iron sulfide serves as the carrier phase for ^{210}Pb in the Cariaco Trench. Particulate iron concentrations are high in the deep water of the Black Sea (LEWIS and LANDING, 1991) and metal sulfides (including pyrite) form in the water column (MURAMOTO et al., 1991; PILSKALN, 1991). This supports the hypothesis that iron sulfide also acts as a carrier phase for the ^{210}Pb in the anoxic layer of the Black Sea.

In contrast to the fate of ^{210}Pb in the oxic layer, particle settling seems to be the limiting factor for the geochemical cycling of ^{210}Pb in the anoxic layer. It takes about 3.6 y for ^{210}Pb to be scavenged onto particulate matter and longer than 8 yrs for adsorbed ^{210}Pb to settle to the bottom sediments. This requires a ^{210}Pb flux of about 16 dpm m^{-2} d^{-1} and a particle settling velocity of about 240 m y^{-1}. This flux is slightly higher than the ^{210}Pb flux measured at the bottom of the euphotic zone (13 dpm m^{-2} d^{-1}) which in turn is assumed to be an indirect estimate of the atmospheric ^{210}Pb flux into the Black Sea. The amount of ^{210}Pb conveyed to the sediments by settling particles is large enough to balance the source from the atmosphere. This conclusion is different from the open ocean where the sinking particles do not carry enough ^{210}Pb to balance the removal fluxes calculated from the ^{210}Pb/^{226}Ra disequilibrium (BACON et al., 1976). BACON et al., 1976) suggested that ^{210}Pb must be transported to ocean boundary sites and scavenged there. The calculations given above suggest that anoxic basins, like the Black Sea, can serve as such boundary scavenging sites.

^{210}Po Scavenging

Polonium is also a particle reactive element, but its geochemical pathways appear to be different from lead. KHARKAR et al. (1976) measured the activities of a number of radionuclides associated with marine zooplankton and found that the degree of enrichment follows the order of Po $\gg$ Pb = Th > Ra > U. FISHER et al. (1983) observed that ^{210}Pb is associated almost exclusively with exterior cellular structural components (cell walls and plasmalemmae), while ^{210}Po is associated with interior cellular organic compounds. As a result, ^{210}Po should be recycled more like a nutrient element. KHARKAR et al. (1976) and FISHER et al. (1983) concluded that polonium behaves more like the nutrient elements. Leaching experiments, carried out by MCKEE (1986), suggested that polonium is preferentially associated with particulate organic carbon, relative to lead. Although polonium has the highest degree of enrichment in zooplankton it also is easily released back to seawater. Field studies by KADKO (1993) support a nutrient-like cycling of ^{210}Po. The case of regenerating ^{210}Po from biological particles typically results in an excess of ^{210}Po relative to ^{210}Pb in the deep ocean. In the Atlantic Ocean, BACON et al. (1976) observed a deficiency of dissolved ^{210}Po, with respect to dissolved ^{210}Pb in the mixed layer, and an enrichment in the thermocline layer. They attributed this to scavenging processes in the surface ocean, followed by regeneration in the subsurface layer.

In the Black Sea the activity of dissolved ^{210}Po is deficient relative to dissolved ^{210}Pb in the euphotic zone and the upper portion of the suboxic zone (Fig. 6). The magnitude of the deficiency of dissolved ^{210}Po in the surface layer is slightly larger at BS3-2 than that at BS3-6. The degree of deviation of dissolved ^{210}Po activity decreases with increasing density at both stations. This indicates preferential scavenging of ^{210}Po over ^{210}Pb by the particles residing in the surface layer, which is consistent with previous work showing the preferential uptake of polonium over lead by planktonic organisms (SHANNON et al., 1970; TUREKIAN et al., 1974; NOZAKI et al., 1976; FISHER et al., 1983).

The residence time of dissolved ^{210}Po calculated from inventories of dissolved ^{210}Po and dissolved ^{210}Pb in the surface layer is about 150 and 230 days for BS3-2 and BS3-6, respectively. A possible explanation for the difference between

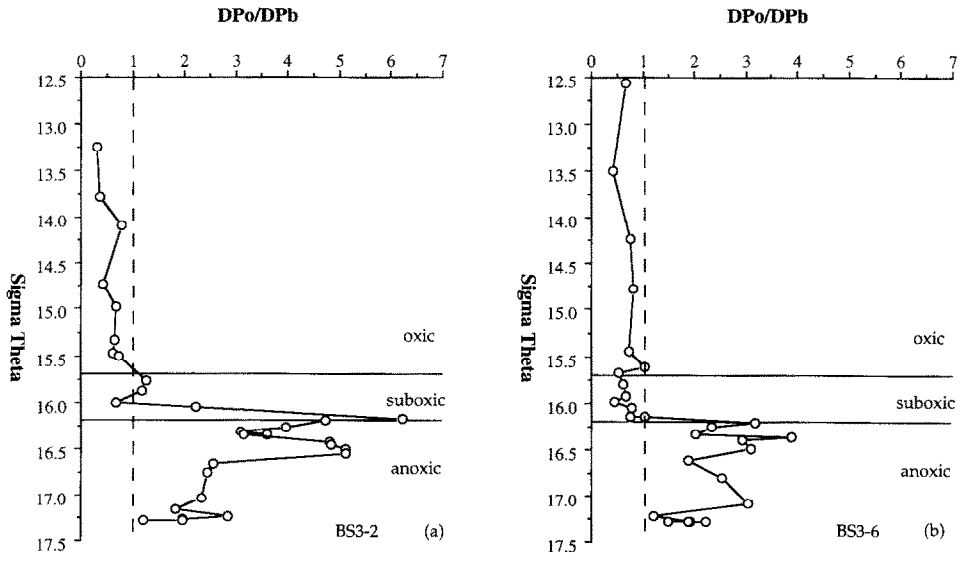

FIG. 6. Vertical distributions vs. density of the ratio of dissolved ^{210}Po to dissolved ^{210}Pb at (a) BS3-2 and (b) BS3-6. The upper and lower boundaries of the suboxic zone are indicated by horizontal lines. The vertical dashed line indicates a ratio of 1.

these two stations is the higher concentration of total suspended matter (Figs. 2, 3). Particulate Mn is about 3–5 times higher, and particulate aluminum is about two times higher in the surface layer of BS3-2, relative to BS3-6 (LEWIS and LANDING, 1991). LEWIS and LANDING (1991) have proposed that these differences are due to the larger influence of fluvial or atmospheric sources at BS3-2, relative to BS3-6.

Particulate ^{210}Po is enriched relative to particulate ^{210}Pb in the euphotic zone of BS3-6, while at BS3-2 it appears to be close to secular equilibrium (Fig. 7). The difference may reflect different particle compositions at the two locations. The suspended particles collected in the euphotic zone of BS3-6 contain twice as much organic carbon than at BS3-2 (RADFORD-KNOERY and CUTTER, 1988). Our ^{210}Po and ^{210}Pb data also suggest that suspended particles from the surface layer of BS3-2 may contain larger amounts of terrestrial particles than at BS3-6. If terrestrial particles, like aluminosilicate minerals, dominate the biogenic particles, then the ^{210}Po/^{210}Pb ratio should be closer to the secular equilibrium value of unity, as observed at BS3-2.

Because ^{210}Po is in excess of ^{210}Pb below the euphotic zone, we cannot apply the scavenging model to calculate residence times. We can calculate the residence time of particulate ^{210}Po, using the trap data. For the upper 150 m the inventories of particulate ^{210}Po at BS3-2 and BS3-6 are 13,030 dpm m^{-2} and 8,058 dpm m^{-2}, respectively. Using the ^{210}Po flux values of 8 dpm m^{-2} d^{-1} and 16.6 dpm m^{-2} d^{-1}, we calculate particulate ^{210}Po residence times of 4.5 y and 1.25 y. These values are similar to the particulate ^{210}Pb residence times given in Table 4.

The activity of dissolved ^{210}Po becomes higher than that of dissolved ^{210}Pb within the suboxic zone at σ_t = 16.0. This excess dissolved ^{210}Po activity seems to be a common feature in anoxic basins (Cariaco Trench: BACON et al., 1980; Orca Basin: TODD et al., 1986; Jellyfish Lake, Palau: BURNETT et al., 1989) and is probably due to regeneration from the particles settling from the surface euphotic zone. However, this regeneration can not explain the large amount of excess ^{210}Po found in the Black Sea. The amount of excess ^{210}Po (about 80×10^3 dpm m^{-2}) requires a source of about 400 dpm m^{-2} d^{-1}. The ^{210}Po flux measured in the drifting traps ranged from 8 to 17 dpm m^{-2} d^{-1}. No ^{210}Po measurements were made on the moored deep trap samples. Apparently, unsupported ^{210}Po must be entering into the central Black Sea from other sources. Since there is no systematic trend of the unsupported dissolved ^{210}Po with depth, we hypothesize that the large area of shelf and slope sediments around the Black Sea may be the main source of excess ^{210}Po in the deep Black Sea.

The value of K_D for ^{210}Po is much greater than ^{210}Pb in the euphotic zone, but the values are similar in the anoxic water. The fluff material at the sediment-water interface is extremely enriched in ^{210}Pb (MOORE and O'NEILL, 1991), but unfortunately, there have been no ^{210}Po analyses on these samples.

A maximum of the ^{210}Po/^{210}Pb ratio in particulate samples is evident in the mid-depth of the suboxic zone of both BS3-2 and BS3-6 (Fig. 7). This peak may be a result of reductive dissolution of particulate Mn in the suboxic zone which releases ^{210}Pb into seawater. Since polonium is preferentially associated with organic phases (MCKEE, 1986), and organic particles are more refractory to reducing conditions than manganese oxyhydroxides, the increase in the ^{210}Po/^{210}Pb particulate ratio in the suboxic zone is due to lower values of particulate ^{210}Pb, caused by release of lead during reductive dissolution of particulate metal oxides.

Inferences from Sediment Trap Experiments

Total mass fluxes measured at BS3-2 are a factor of 2–4 higher than those at BS3-6 (Fig. 4). Unlike the total mass fluxes, the ^{210}Pb fluxes show little variation between the two

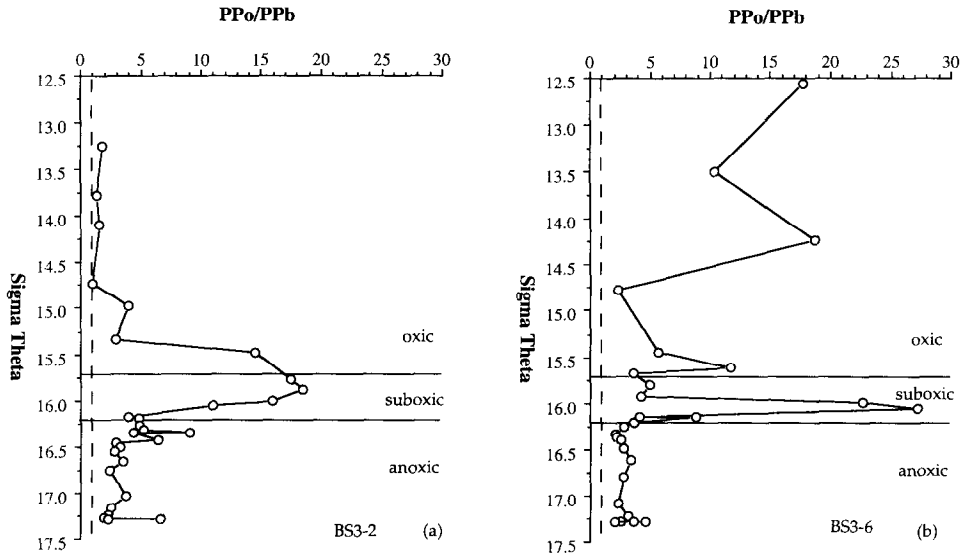

FIG. 7. Vertical distributions vs. density of the ratio of particulate ^{210}Po to particulate ^{210}Pb at (a) BS3-2 and (b) BS3-6. The upper and lower boundaries of the suboxic zone are indicated by horizontal lines. The vertical dashed line indicates a ratio of 1.

stations (Fig. 4). This is consistent with the net fluxes estimated from the $^{210}Pb/^{226}Ra$ disequilibria in the water column, which also showed no difference between the two stations. The correlation between the ^{234}Th flux and total mass flux, reported previously (WEI and MURRAY, 1992), is not found between the ^{210}Pb flux and total mass flux. The lack of correlation between ^{210}Pb flux and total mass flux is also observed in the open ocean (HARADA and TSUNOGAI, 1986). The ^{210}Pb flux decreases monotonically from 13 dpm m^{-2} d^{-1} at the base of the euphotic zone to about 9 dpm m^{-2} d^{-1} at 150 m. This decrease implies that settling particles disaggregate into smaller particles, or that the ^{210}Pb associated with the settling particles is desorbed into seawater because of the presence of dissolved sulfide.

The specific activities of ^{210}Pb in the settling particles collected by the two shallower traps (Table 3) are similar to those of suspended particles. However, the suspended particles in the vicinity of 150 m have substantially higher ^{210}Pb-specific activities than the trap particles (300–400 dpm g^{-1} vs. 20–90 dpm g^{-1}). This suggests that the particles that settle into the anoxic zone of the Black Sea are formed at shallower depths in the water column.

Even though there is no correlation between the total mass flux and the ^{210}Pb flux, the specific ^{210}Pb activity decreases exponentially as the mass flux increases (Fig. 8). A similar correlation was also found in the open ocean (HARADA and TSUNOGAI, 1986). The concentration of ^{210}Pb associated with settling particles may be determined by the residence time of the particles. In other words, the longer the settling particles are in contact with seawater, the more ^{210}Pb can be scavenged. The same argument may also be true for ^{210}Po.

The ^{210}Po flux results show some interesting features (Fig. 4). First, the ^{210}Po fluxes measured at all three depths of BS3-6 are higher than those of BS3-2, while the total mass fluxes have the opposite relationship. Second, the specific ^{210}Po activities of trap particles increase with depth (Table 3). The specific ^{210}Po activities of trap particles collected at BS3-6 is about 2–7 times higher than those at BS3-2. Third, except for the particles collected by the shallowest trap (36 m) at BS3-2, trap particles have a significantly lower specific ^{210}Po activity than suspended particles found at the same depths (Table 3 vs. Table 2). Fourth, the range of $^{210}Po/^{210}Pb$ ratios in trap particles (0.68–1.71) is much smaller than that of suspended particles (0.5–28) (Table 3 vs. Fig. 7).

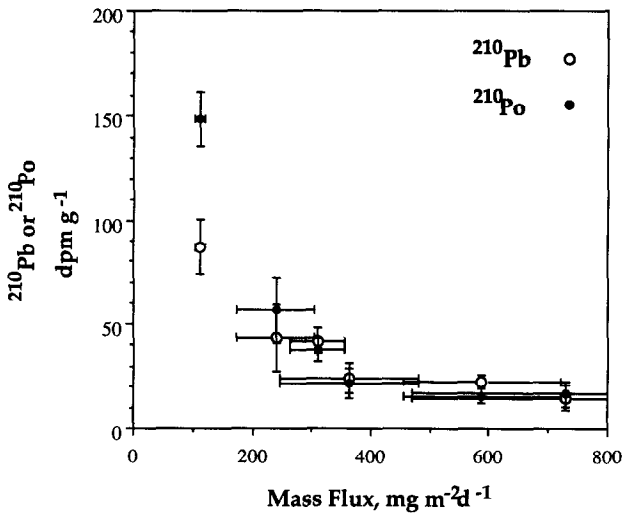

FIG. 8. Correlation between the specific activities (dpm g^{-1}) of ^{210}Pb (open circles) and ^{210}Po (solid circles) of trap particles and the total mass fluxes.

Comparative Geochemistries of ^{210}Pb, ^{210}Po, and ^{234}Th

Vertical variations of the distribution coefficients of ^{210}Pb, ^{210}Po, and ^{234}Th defined as

$$K_D = \frac{[\text{Me}]\text{part}}{[\text{Me}]\text{diss}\ C_p},$$

where

[Me]part = activities of particulate ^{210}Pb, ^{210}Po (dpm 100 L^{-1}), and ^{234}Th (dpm L^{-1}),
[Me]diss = activities of dissolved ^{210}Pb, ^{210}Po (dpm 100 L^{-1}), and ^{234}Th (dpm L^{-1}),
C_p = TSM concentration (g mL^{-1}),

are plotted in Fig. 9. The ratio of distribution coefficients of ^{210}Po and ^{234}Th relative to those of ^{210}Pb are plotted vs. depth in Fig. 10. Since the K_D values can serve as a measure of reactivity of a metal with particles, the vertical profiles of K_D are useful for describing the interaction of Th, Pb, and Po with particles of different composition.

In general, K_D values of ^{210}Pb and ^{210}Po increase from the oxic euphotic zone to the anoxic deep water. These K_D values are smaller in the surface layer of BS3-2 than at BS3-6. The suspended particles in the surface layer at BS3-2, which probably contain more terrestrial particles, are less reactive to both ^{210}Pb and ^{210}Po. The ratio of K_D values of ^{210}Po to ^{210}Pb in the surface layer is larger than unity, which implies that ^{210}Po is preferentially scavenged by the particles residing in the euphotic zone.

The K_D values of ^{234}Th in the surface euphotic zone (WEI and MURRAY, 1992) are about 10^6 mL g^{-1} at both stations. The values from thorium do not vary as much as those for lead and polonium, suggesting that thorium scavenging may be less dependent on the composition of particles. Except for a few data points in the euphotic zone of BS3-2, the K_D values for ^{210}Po are always 10–100 times larger than for ^{234}Th. The K_D values for ^{210}Pb are similar to ^{234}Th in the oxic and suboxic zones, and are similar to ^{210}Po in the anoxic zone.

K_D values of both ^{210}Pb and ^{210}Po (and to a lesser extent ^{234}Th) increase to a maximum at the mid-depth of the suboxic zone (σ_t = 15.5 to 16.0), then decrease to slight minimum in the lower layer of the suboxic zone (σ_t = 16.0 for ^{210}Pb; σ_t = 16.2 for ^{210}Po). The redox cycling of manganese and iron metal oxides across the oxic-anoxic transitional layer may be responsible for this variation, because the depth of the maxima coincide with the depth of maximum particulate manganese and iron.

In the deep H_2S zone, both ^{210}Pb and ^{210}Po have similar K_D values of about 10^8 mL g^{-1}. The formation of metal sulfide minerals is probably the cause of the high K_D of ^{210}Pb. Lead has well known class B metal tendencies (STUMM and MORGAN, 1981). Higher affinity of B-type metal cations for sulfide particles was confirmed by adsorption experiments

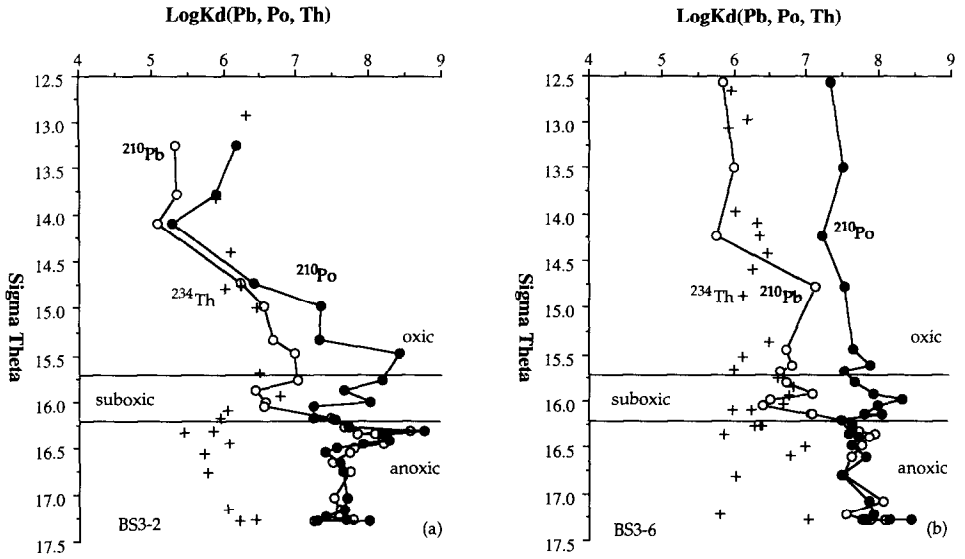

FIG. 9. Vertical profiles vs. density of the distribution coefficients (K_D) of ^{210}Pb (open circles), ^{210}Po (solid circles), and ^{234}Th (crosses) at (a) BS3-2 and (b) BS3-6. The upper and lower boundaries of the suboxic zone are indicated by horizontal lines.

using H_2S-containing Cariaco Trench sediments (LI et al., 1984). The similarity between the K_D values for ^{210}Pb and ^{210}Po suggest that ^{210}Po may also form or adsorb on sulfide phases. Polonium is thought to have transition metal characteristics, although its chemical properties are less well known (COTTON and WILKINSON, 1966). Thorium is known to be a class A metal (STUMM and MORGAN, 1981) and has a lower affinity for sulfidic ligands. As a result ^{234}Th has a lower K_D value than ^{210}Pb and ^{210}Po. The relative partitioning of ^{210}Pb, ^{210}Po, and ^{234}Th to particles residing in different regimes of the water column are shown in Table 5.

While high TSM concentrations tend to be in the oxic zone and low TSM concentrations in the anoxic zone, the total range of TSM concentration is only about 10^2. Nevertheless, good correlations are observed between TSM and the K_D values for ^{234}Th, ^{210}Pb, and ^{210}Po (Fig. 11). The correlation for the anoxic samples (closed symbols) are significantly different from the oxic/suboxic samples (open symbols). The respective regressions and values of r^2 are given in the caption for Fig. 11. In all cases, the correlations are worse if the anoxic and oxic/suboxic samples are not distinguished.

There are interesting patterns in these correlations. The slopes of the TSM correlations for ^{234}Th, ^{210}Pb, and ^{210}Po in the anoxic, sulfidic water are the same within the errors of the analysis (-1.04 ± 0.13 for Th, -0.86 ± 0.16 for Pb, and

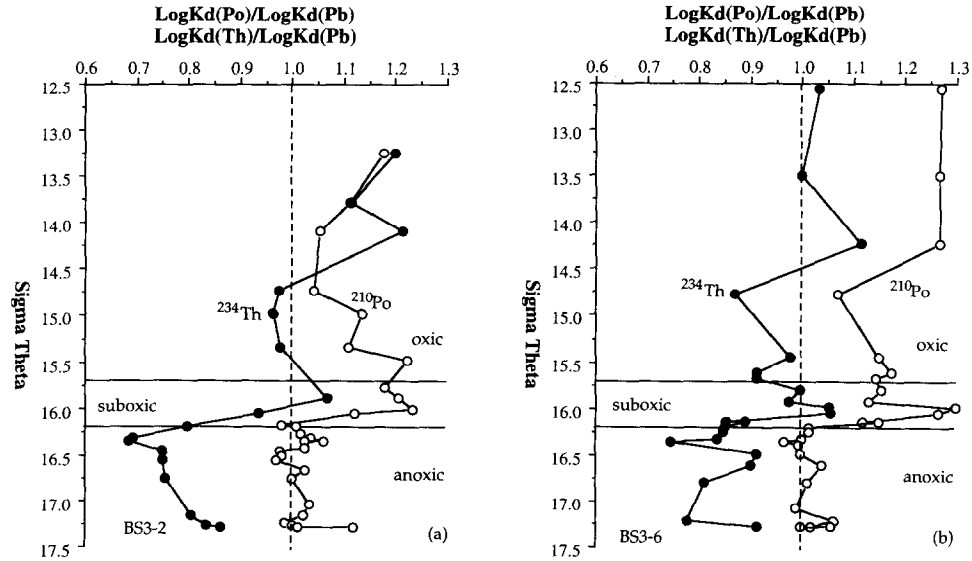

FIG. 10. Vertical profiles vs. density of the ratio of the distribution coefficients of ^{210}Po (open circles) and ^{234}Th (crosses) relative to the distribution coefficients of ^{210}Pb at (a) BS3-2 and (b) BS3-6. The upper and lower boundaries of the suboxic zone are indicated by horizontal lines.

Table 5. Relative affinities of thorium, lead, and polonium to the particles found in different regimes of the Black Sea water column.

Zones	BS3-2	BS3-6
Oxic	Po~Th>Pb	Po>Th~Pb
Upper Suboxic	Po>Th~Pb	Po>Th~Pb
Lower Suboxic	Po~Pb>Th	Po~Pb>Th
Anoxic	Po~Pb>Th	Po~Pb>Th

-1.14 ± 0.16 for Po). The TSM correlations in the oxic/suboxic zones are more variable (-0.50 ± 0.11 for Th, -1.63 ± 0.37 for Pb, and -2.15 ± 0.34 for Po).

Negative log K_D − log TSM correlations have been previously been observed in laboratory and field data for ^{234}Th, ^{7}Be, and other elements (LI et al., 1984; MCKEE, 1986; HONEYMAN et al., 1988; HONEYMAN and SANTSCHI, 1989). Several hypotheses have been proposed for this particle concentration effect (MOREL and GSCHWEND, 1987) but it appears most likely that coagulation of colloidal size particles plays an important role.

HONEYMAN and SANTSCHI (1989) used the correlation of TSM and ^{234}Th in oceanic data to derive a relationship between the mass concentration of colloids (C_p^*) and the mass concentration of filterable particles (C_p) expressed as log $C_p^* = 0.7 \log C_p - 2.6$. A similar correlation of TSM and ^{7}Be in mostly freshwater data led to a relation with a slightly different slope of log $C_p^* = 0.5 \log C_p - 2.3$. The dependency of C_p^* on C_p derived from the Black Sea ^{234}Th, ^{210}Pb, and ^{210}Po data are summarized in Table 6. The slopes for ^{234}Th, ^{210}Pb, and ^{210}Po in the sulfidic regime are similar, at about 1.0 ± 0.1. In the oxic/suboxic regimes the slopes are quite different. The Black Sea ^{234}Th data suggest a square root dependency ($C_p^* = f(C_p^{0.5})$) similar to the ^{7}Be-based relation of HONEYMAN and SANTSCHI (1989), but is probably also not statistically different from their slope for ^{234}Th ($C_p^* = f(C_p^{0.7})$). The oxic/suboxic ^{210}Pb- and ^{210}Po-derived relations are different from ^{234}Th, but overlap statistically with each other. Their relationships suggest that the concentrations of colloids increase faster than the concentration of filterable particles (approximately $C_p^* = f(C_p^{2.0})$).

According to the Brownian pumping model, the particle coagulation rate and the concentration of colloids (C_p^*) should be the same for all metals in a given system (HONEYMAN and SANTSCHI, 1992). The chemical differences between elements are expressed as the adsorption density (Γ_c) on colloids, which in turn is a function of the conditional sorption constant on colloids (K_c) and the total dissolved metal concentration. The fact that the C_p^*/C_p relations should be the same, but differ for ^{234}Th, ^{210}Pb, and ^{210}Po in the oxic/suboxic zone, suggests that the values of the conditional sorption constants on colloids (K_c) and the filterable particles (K_{pc}) vary for these three metals. The relations in Table 6 were derived from the plots of the different elements which means that they reflect the chemical differences of these three elements. HONEYMAN and SANTSCHI (1989) show that K_{pc} is equal to the constant value of K_D observed at low concentrations of C_p. The value of K_{pc} derived in their analysis for Th (about $10^{7.0}$) is consistent with our Black Sea ^{234}Th data. The values of K_{pc} for ^{210}Pb and ^{210}Po in the Black Sea must be greater than $10^{8.0}$ (Fig. 11). The differences in K_{pc} for these three metals may reflect the roles oxide and sulfide precipitation play in influencing the distribution of ^{210}Pb and ^{210}Po.

These results are intriguing, but are based on a small range in TSM or C_p. There have not been the necessary studies needed to quantitatively interpret these results. These include studies of colloidal interaction with metals of different reac-

Table 6 The relationship between the mass off colloidal particles (C^*_P) and the mass of filterable particles (C_P) derived from the correlations of ^{234}Th, ^{210}Pb and ^{210}Po with TSM (after Honeyman and Santschi, 1989)

^{234}Th	Sulfidic	$C_p^* = 1.04(\pm0.13)\ C_p + 1.56\ (\pm0.97)$
	oxic/suboxic	$C_p^* = 0.50(\pm0.11)\ C_p - 2.76\ (\pm0.77)$
^{210}Pb	Sulfidic	$C_p^* = 0.86(\pm0.16)\ C_p - 1.41\ (\pm1.16)$
	oxic/suboxic	$C_p^* = 1.63(\pm0.37)\ C_p + 4.84\ (\pm2.55)$
^{210}Po	Sulfidic	$C_p^* = 1.14(\pm0.16)\ C_p + 0.56\ (\pm1.19)$
	oxic/suboxic	$C_p^* = 2.15(\pm0.34)\ C_p + 7.57\ (\pm2.38)$

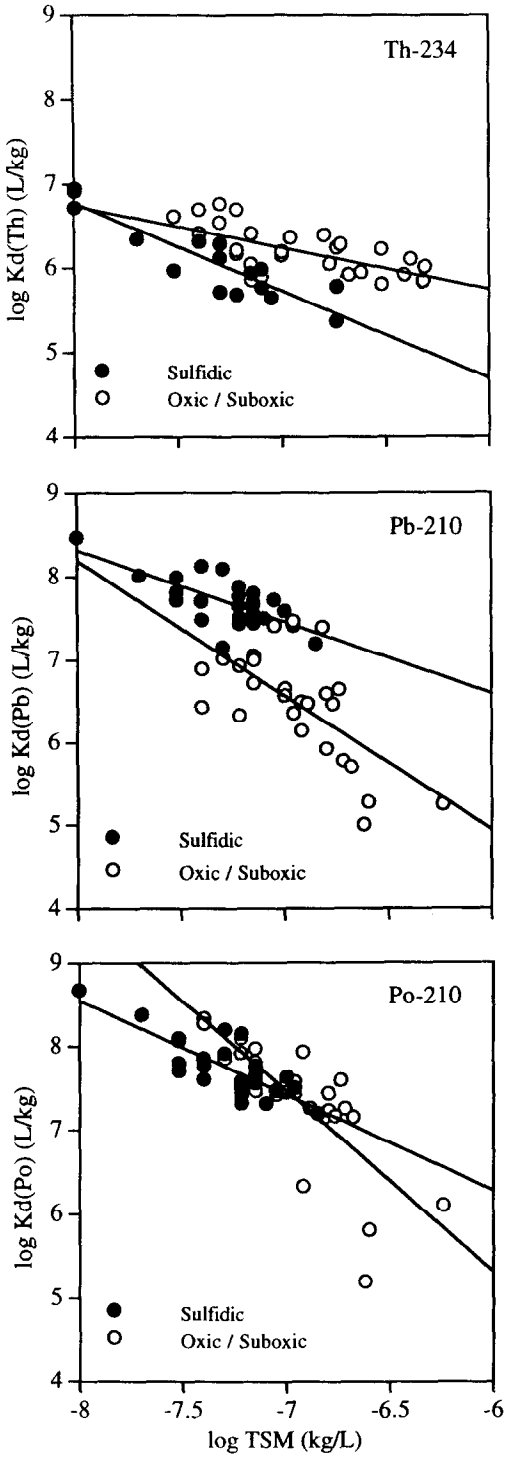

FIG. 11. Correlation between the log TSM concentration and the log distribution coefficients of ^{234}Th, ^{210}Pb, and ^{210}Po. The solid symbols are from the anoxic, sulfidic zone. The open symbols are from the oxic/suboxic zones. The lines represent the following regressions:

^{234}Th	Sulfidic	log K_D (Th) = -1.04 ± 0.13TSM $- 1.55 \pm 0.93$ $r^2 = 0.82$,
	oxic/suboxic	log K_D (Th) = -0.50 ± 0.11TSM $+ 2.76 \pm 0.77$ $r^2 = 0.43$,
^{210}Pb	Sulfidic	log K_D (Pb) = -0.86 ± 0.16TSM $+ 1.41 \pm 1.16$ $r^2 = 0.52$,
	oxic/suboxic	log K_D (Pb) = -1.63 ± 0.37TSM $- 4.83 \pm 2.6$ $r^2 = 0.44$,
^{210}Po	Sulfidic	log K_D (Po) = -1.14 ± 0.16TSM $- 0.56 \pm 1.19$ $r^2 = 0.64$,
	oxic/suboxic	log K_D (Po) = -2.15 ± 0.34TSM $- 7.57 \pm 2.38$ $r^2 = 0.61$.

tivities and metal interaction with colloids of different composition. Direct measurements of the colloidal concentrations of these metals should be conducted to test these results and to fully understand the scavenging mechanisms. We also need to use independent estimates of C_p^*, using approaches not based on metals of different reactivity.

CONCLUSIONS

The following conclusions can be made about the distribution of dissolved and particulate ^{210}Pb and ^{210}Po in the water column and the vertical fluxes of ^{210}Pb and ^{210}Po in the upper 150 m of the Black Sea.

1) The distributions of dissolved and particulate ^{210}Pb and ^{210}Po from two stations in the Black Sea show regional differences in the euphotic zone and upper suboxic zone, but compare very closely in the deeper part of the suboxic zone and anoxic zone when plotted vs. density rather than depth.
2) The distributions of ^{210}Pb are controlled by the redox conditions in the water column. In the oxic and suboxic zones, ^{210}Pb is mainly in the dissolved form, while particulate ^{210}Pb dominates in the anoxic zone. The ratio of particulate ^{210}Pb to dissolved ^{210}Pb increases to greater than 1 at the suboxic/anoxic boundary. The data suggest that metal oxides play a role in scavenging ^{210}Pb in the suboxic zone, but it is not possible to identify the relative importance of Mn versus Fe oxides. Interaction with sulfide probably controls the distribution of ^{210}Pb in the anoxic zone.
3) The distribution of ^{210}Po tends to be dominated by the particulate fraction in both the suboxic and anoxic zones. The deficiency of dissolved ^{210}Pb relative to dissolved ^{210}Pb in the euphotic zone indicates preferential scavenging of ^{210}Po relative to ^{210}Pb by organisms. Dissolved ^{210}Po is greater than dissolved ^{210}Pb in the deep suboxic and anoxic zones. This unsupported ^{210}Po can not be supported by the ^{210}Po flux measured by drifting traps. We hypothesize that the source of excess ^{210}Po must be the large area of shelf and slope sediments.
4) The residence times of dissolved (DPb) and particulate (PPb) ^{210}Pb in the oxic, suboxic, and anoxic layers of the Black Sea were calculated using a simple scavenging model. Both τDPb and τPPb increase with depth from about 1 and 0.1 y in the oxic layer to 3.6 and 8.5 y in the anoxic layer, respectively. The short residence times suggest that the Black Sea is an effective sink for ^{210}Pb. Based on the ^{210}Pb/^{226}Ra disequilibrium in the anoxic layer of the Black Sea, we obtained a flux of ^{210}Pb via particle settling to the sediments of about 16 dpm m^{-2} d^{-1}, and a particle settling velocity of about 240 m y^{-1}.
5) The vertical fluxes of ^{210}Pb and ^{210}Po in the upper 150 m measured by sediment traps range from 9 to 13 dpm m^{-2} d^{-1} and from 8 to 16 dpm m^{-2} d^{-1}, respectively. The ^{210}Pb fluxes are remarkably similar at the two stations

while the ^{210}Po fluxes at BS3-2 are significantly less than at BS3-6. The total mass fluxes are about 2–4 times higher at BS3-2 than at BS3-6.

6) By comparing the distribution coefficients (K_D) of ^{210}Pb, ^{210}Po, and ^{234}Th, we conclude that polonium has the highest affinity for particles in the euphotic zone, and thorium is the least reactive to the sulfidic particles in the anoxic layer of the Black Sea.

7) K_D values for ^{234}Th, ^{210}Pb, and ^{210}Po decrease with increasing total suspended matter, and the relationships are different for the anoxic and oxic/suboxic zones. These results are consistent with the hypothesis that colloidal phases play an important role in controlling the distributions.

Acknowledgments—We are grateful for the help given by G. White and B. Paul in sampling. We thank H. Jannasch for assisting with the sediment trap samples, and Dr. C.-A. Huh for kindly alpha counting some samples. Jeff Berry conducted the colloidal calculations. Laurie Balistrieri, Peter Santschi, Brent McKee, and Ken Buesseler reviewed the manuscript. Support for this research was provided by NSF grant number NSF OCE 8511580 and Taiwan National Science Council Grant NSC 82-0209-M-002A-021-K. This manuscript is contribution No. 1967 from the School of Oceanography, University of Washington, and contribution No. 014 of the CoMSBlack Project.

Editorial handling: R. C. Aller

REFERENCES

ANDERSON R. F. and FLEER A. P. (1982) Determination of natural Actinides and plutonium in marine particulate material. *Anal. Chem.* **54,** 1142–1147.

BACON M. P., SPENCER D. W., and BREWER P. G. (1976) ^{210}Pb/^{210}Ra and ^{210}Po/^{210}Pb disequilibria in seawater and suspended particulate matter. *Earth Planet. Sci. Lett.* **32,** 277–299.

BACON M. P., BREWER P. G., SPENCER D. W., MURRAY J. W., and GODDARD J. (1980) Lead-210, polonium-210, manganese, and iron in the Cariaco Trench. *Deep-Sea Res.* **27,** 119–135.

BUESSELER K. O. (1991) Do upper-ocean sediment traps provide an accurate record of particle flux? *Nature* **353,** 420–423.

BUESSELER K. O., LIVINGSTON, H. D., and CASSO S. A. (1991) Mixing between oxic and anoxic waters of the Black Sea as traced by Chernobyl cesium isotopes. *Deep-Sea Res.* **38,** S725–S745.

BURNETT W. C., LANDING W. M., LYONS W. B., and DREM W. (1989) Jellyfish Lake, Palau—a model anoxic environment for geochemical studies. *Eos* **70,** 777.

CHUNG Y. and CRAIG H. (1983) Pb in the Pacific: the GEOSECS measurements of particulate and dissolved concentration. *Earth Planet. Sci. Lett.* **65,** 406–432.

COCHRAN J. K., BACON M. P., KRISHNASWAMI S., and TUREKIAN K. K. (1983) ^{210}Po and ^{210}Pb distributions in the central and Eastern Indian Ocean. *Earth Planet. Sci. Lett.* **65,** 433–452.

CODISPOTI L. A., FRIEDERICH G. E., MURRAY J. W., and SAKAMOTO C. (1994) Chemical variability in the Black Sea: Implications of data obtained with a continuous vertical profiling system that penetrated the oxic/anoxic interface. *Deep-Sea Res.* (in press).

COTTON R. A. and WILKENSON G. (1966) *Advanced Inorganic Chemistry.* Wiley.

CRAIG H., KRISHNASWAMI S., and SOMAJAJULU B. L. K. (1973) ^{210}Pb-^{226}Ra: Radioactive disequilibrium in the deep sea. *Earth Planet. Sci. Lett.* **17,** 295–305.

FISHER N. S., BURNS K. A., CHERRY R. D., and HEYRAUD M. (1983) Accumulation and cellular distribution of ^{241}Am, ^{210}Pb, and ^{210}Po in two marine algae. *Mar. Ecol. Prog. Series 11,* pp. 233–237.

FLYNN W. W. (1968) The determination of low levels of polonium-210 in environmental materials. *Anal. Chim. Acta* **43,** 221–227.

HARADA K. and TSUNOGAI S. (1986) Fluxes of ^{234}Th, ^{210}Po and ^{210}Pb determined by sediment trap experiments in pelagic oceans. *J. Oceanogr. Soc. Japan* **42,** 192–200.

HARADA K., BURNETT W. C., LAROCK P. A., and COWART J. B. (1989) Polonium in Florida groundwater and its possible relationship to the sulfur cycle and bacteria. *Geochim. Cosmochim. Acta* **53,** 143–150.

HONEYMAN B. D. and SANTSCHI P. H. (1989) A Brownian pumping model for ocean trace metal scavenging: Evidence from Th isotopes. *J. Mar. Res.* **47,** 951–992.

HONEYMAN B. D. and SANTSCHI P. H. (1992) The role of particles and colloids in the transport of radionuclides and trace metals in the oceans. In *Environmental Particles* (ed. J. BUFFLE et al.), Vol. 1, pp. 379–423. Lewis.

HONEYMAN B. D., BALISTRIERI L. S., and MURRAY J. W. (1988) Oceanic trace metal scavenging: the importance of particle concentration. *Deep-Sea Res.* **35,** 227–246.

JANNASCH H. W. (1989) Trace metal behavior in the upper water column: A case study in the Galapagos Front. Ph.D. dissertation, Univ. Washington.

KADKO D. (1993) Excess ^{210}Po and nutrient cycling within the California coastal transition zone. *J. Geophys. Res.* **98,** 857–864.

KEMPE S., DIERCKS A. R., LIEBEZEIT G., and PRANGE A. (1991) Geochemical and structural aspects of the pycnocline in the Black Sea (R/V Knorr 134-8 Leg 1, 1988). In *Black Sea Oceanography* (ed. E. IZDAR et al.), pp. 89–110. Kluwer.

KHARKAR D. P., THOMSON J., TUREKIAN K. K., and FORSTER W. O. (1976) Uranium and thorium decay series nuclides in plankton from the Caribbean. *Limnol. Oceanogr.* **21,** 294–299.

KNAUER G. A., MARTIN J. H., and BRULAND K. W. (1979) Fluxes of particulate carbon, nitrogen and phosphorus in the upper water column of the northeast Pacific. *Deep-Sea Res.* **26,** 97–108.

KRISHINASWAMI S., LAL D., SOMAYAJULU B. L. K., WEISS R. F., and CRAIG H. (1976) Large volume in situ filtration of deep Pacific waters: Mineralogical and radioisotope studies. *Earth Planet. Sci. Lett.* **32,** 420–429.

LEWIS B. L. and LANDING W. M. (1991) The biogeochemistry of manganese and iron in the Black Sea. *Deep-Sea Res.* **38,** S773–S804.

LI Y.-H., BURKHARDT L., BUCHHOLTZ M., O'HARA P., and SANTSCHI P. H. (1984) Partition of radiotracers between suspended particles and seawater. *Geochim. Cosmochim. Acta* **48,** 2011–2019.

MARTIN J. H., KNAUER G. A., KARL D. M., and BROENKOW W. W. (1987) VERTEX, carbon cycling in the northeast Pacific. *Deep-Sea Res.* **34,** 267–285.

MCKEE B. A. (1986) The fate of particle-reactive radionuclides in the Amazon and Yangtze continental shelves. Ph.D. dissertation, North Carolina State Univ.

MOORE W. S. (1976) Sampling ^{226}Ra in the deep ocean. *Deep Sea Res.* **23,** 647–651.

MOORE W. S. and O'NEILL D. J. (1991) Radionuclide distributions in recent Black Sea sediments. In *Black Sea Oceanography* (ed. E. IZDAR et al.), pp. 257–270. Kluwer.

MOREL F. M. M. and GSCHWEND P. M. (1987) The role of colloids in the partitioning of solutes in natural waters. In *Aquatic Surface Chemistry* (ed. W. STUMM), pp. 405–493. Wiley.

MURRAY J. W. et al. (1989) Unexpected changes in the oxic/anoxic interface in the Black Sea. *Nature* **338,** 411–413.

MURRAY J. W., CODISPOTI L. A., and FRIEDERICH G. E. (1994) Redox Environments: The suboxic zone in the Black Sea. In *Aquatic Chemistry* (ed. C. P. HUANG et al.), *Advances in Chemistry Series,* (in press). ACS.

NOZAKI Y. and TSUNOGAI S. (1976) ^{226}Ra, ^{210}Pb and ^{210}Po disequilibria in the Western North Pacific. *Earth Planet. Sci. Lett.* **32,** 313–321.

NOZAKI Y., THOMSON J., and TUREKIAN K. K. (1976) The distribution of ^{210}Pb and ^{210}Po in the surface waters of the Pacific Ocean. *Earth Planet. Sci. Lett.* **32,** 304–312.

O'NEILL D. J., TODD J. F., and MOORE W. S. (1992) ^{226}Ra in the Black Sea and the Sea of Marmara. *Earth Planet. Sci. Lett.* **110,** 7–21.

RADFORD-KNOERY J. and CUTTER G. A. (1988) Particulate nitrogen and carbon in the Black Sea. *Eos,* **69,** 1240.

RAMA, KOIDE M., and GOLDBERG E. D. (1961) Lead-210 in natural waters. *Science* **134,** 98–99.

SAYDAM C., TUGRUL S., BASTURK O., and OGUZ T. (1993) Identification of the oxic/anoxic interface by isopycnal surfaces in the Black Sea. *Deep-Sea Res.* **40,** 1405–1412.

SHANNON L. V., CHERRY R. D., and ORREN M. J. (1970) Polonium-210 and lead-210 in the marine environment. *Geochim. Cosmochim. Acta* **34,** 701–711.

SPENCER D. W. and BREWER P. G. (1971) Vertical advection diffusion and redox potentials as controls on the distribution of manganese and other trace metals dissolved in waters of the Black Sea. *J. Geophy. Res.* **76,** 5877–5892.

SPENCER D. W., BREWER P. G., and SACHS P. L. (1972) Aspects of the distribution and trace element composition of suspended matter in the Black Sea. *Geochim. Cosmochim. Acta* **36,** 71–86.

SPENCER D. W., BACON M. P., and BREWER P. G. (1980) The distribution of ^{210}Pb and ^{210}Po in the North Sea. *Thal. Yugoslavica* **16,** 125–154.

SPENCER D. W., BACON M. P., and BREWER P. G. (1981) Models of the distribution of ^{210}Pb in a section across the North Equatorial Atlantic Ocean. *J. Mar. Res.* **39,** 119–138.

STUMM W. and MORGAN J. J. (1981) *Aquatic Chemistry.* Wiley.

TEBO B. M. (1991) Manganese (II) oxidation in the suboxic zone of the Black Sea. *Deep-Sea Res.* **38,** S883–S905.

TEBO B. M., ROSSON R. A., and NEALSON K. H. (1991) Potential for manganese (II) oxidation and manganese (IV) reduction to co-occur in the suboxic zone of the Black Sea. In *Black Sea Oceanography* (ed. E. IZDAR et al.), pp. 173–186. Kluwer.

TODD J. F., WONG G. T.-F., and REID D. F. (1986) The geochemistries of ^{210}Po and ^{210}Pb in waters overlying and within the Orca Basin, Gulf of Mexico. *Deep-Sea Res.* **33,** 1293–1306.

TSUNOGAI S. and NOZAKI Y. (1971) Lead-210 and polonium-210 in the surface water of the Pacific. *Geochem. J.* **5,** 165–173.

TSUNOGAI S., NOZAKI Y., and MINAGAWA M. (1974) Behavior of heavy metals and particulate matters in seawater expected from that of radioactive nuclides. *J. Oceanogr. Soc. Japan* **30,** 251–259.

TUGRUL S., BASTURK O., SAYDAM C., and YILMAZ A. (1992) Changes in the hydrochemistry of the Black Sea inferred from water density profiles. *Nature* **359,** 137–139.

TUREKIAN K. K., KHARKER D. P., and THOMSON J. (1974) The fates of ^{210}Pb and ^{210}Po in the ocean surface. *J. Res. Atm.,* 639–646.

TUREKIAN K. K., NOZAKI Y., and BENNIGER L. K. (1977) Geochemistry of atmospheric radon and radon products. *Ann. Rev. Earth Planet. Sci.* **5,** 227–255.

VINOGRADOV M. YA. (1991) The upper boundary of the hydrogen sulfide zone in the Black Sea and trends in position. *Oceanology* **31,** 299–303.

VINOGRADOV M. YE and NALBANDOV YU. R. (1990) Effect of changes in water density on the profiles of physiochemical and biological characteristics in the pelagic ecosystem of the Black Sea. *Oceanology* **30,** 567–573.

WEI C.-L. (1990) Studies of marine scavenging by naturally occurring radionuclides. Ph.D. dissertation, Univ. Washington.

WEI C.-L. and MURRAY J. W. (1992) 234Th/238U disequilibria in the Black Sea. *Deep-Sea Res.* **38,** S855–S873.

WHITE G., RELANDER M., POSTEL J., and MURRAY J. W. (1989) Hydrographic data from the 1988 Black Sea Oceanographic Expedition. *Univ. Washington Spec. Rept. No. 109.*